Journal of
Nanoscience and Nanotechnology
Vol. 12, 1–8, 2012

Prussian Blue Modified Ferritin as Peroxidase Mimetics and Its Applications in Biological Detection

Wei Zhang[1], Yu Zhang[1,*], Yanhua Chen[1], Suyi Li[2], Ning Gu[1,*], Sunling Hu[1], Ying Sun[1], Xue Chen[1], and Quan Li[1]

[1]*State Key Laboratory of Bioelectronics, Jiangsu Key Laboratory for Biomaterials and Devices, School of Biological Science and Medical Engineering, Southeast University, Nanjing 210096, P. R. China*
[2]*Zhongda Hospital, Southeast University, Nanjing 210096, P. R. China*

Ferritins are natural nanoscale structures composed with 24 subunits endowed with similar three-dimensional structures. The iron is stored in the form of ferrihydrite phosphate in the hollow spherical ferritin shells. Prussian blue nanoparticles (PBNPs) have been certified a kind of mimetic enzyme with the advantages of stability, high catalytic activity and low prices. In this context, we designed a strategy to synthesize PBNPs of small size using ferritin as template and meanwhile retain the biological properties of ferritin. Our results show the resulting nanostructures (Prussian blue modified ferritin nanoparticles, PB-Ft NPs) got very small size and relatively high catalytic activity, furthermore, PB-Ft NPs successfully combined the intrinsic enzyme mimetic activity of PBNPs and the specificity of ferritin. Peroxidase-like activity which fits well the Michaelis–Menten kinetics was found strongly depending on pH, temperature and the concentration of PB-Ft NPs. Then a sensitive method for glucose detection was developed using glucose oxidase (GOx) and PB-Ft NPs. The consequence of Enzyme-linked immunosorbent assay (ELISA) shows PB-Ft NPs possess both specificity and peroxidase-like activity, which suggests that PB-Ft NPs can be served as a useful reagent in some biological detections.

Keywords: Prussian Blue (PB), Ferritin, Peroxidase, ELISA, Glucose Detection.

RESEARCH ARTICLE

1. INTRODUCTION

Various nanoparticles have shown great promise in the field of biomedical and biosensing applications.[1–7] Among them, Prussian blue nanoparticles (PBNPs) have been increasingly noted in the field of mimetic enzyme, it is usually considered as an "artificial enzyme peroxidase" because of its high surface activity and selectivity towards the reduction of hydrogen peroxide and oxygen, and it has been extensively used in the construction of electrochemical biosensors.[8–11] In our previous work, PB modified Fe_2O_3 magnetic nanoparticles (PBMNPs) were synthesized and demonstrated to have very high peroxidase-like activity,[9] due to the low redox potential and excellent electron transfer capability. And PBMNPs-SPA (staphylococcal protein A) conjugates were further constructed for ELISA detection.

Ferritin is the cell's storage compartment for iron from plants and animals to bacteria and archaea. It is a native nanoscale structure with specific biological functions. A molecule of ferritin is usually composed of 24 subunits that form a hollow spherical shell of 8 nm in inner diameter which encases a core of up to 4500 Fe (III) atoms.[12–14] Structural features of ferritins from humans, horse, bullfrog and bacteria are all essentially the same architecture in spite of large variations in primary structure,[15] so ferritin from other organisms may have the same functions as human ferritin. Many nanoparticles, such as gold cluster[17] and platinum nanoparticles (PtNPs),[21] have been synthesized using ferritins as nano-reactors through ferritin-loading approach[16–21] and assembly-disassembly approach.[22,23]

It is well known that Prussian blue staining is always used to indicate the presence of iron in the tissues[24–28] and the uptake of iron oxide nanoparticles in cells,[29–34] since ferric iron can readily react with the ferrocyanide in acidic condition, resulting in the formation of a bright blue pigment namely Prussian blue. From this, herein we report a simple method to synthesize PBNPs of very small size taking use of the nature nanostructure of horse spleen ferritin (HoSF) as template, where the PBNPs was synthesized by the reaction of ferrocyanide with the ferric iron at the surface of the iron oxide cores and deposited on the

*Author to whom correspondence should be addressed.

cores thus providing relatively high enzyme mimetic activity; meanwhile, we intended to preserve the function of ferritin in the Prussian blue modified ferritin nanoparticles (PB-Ft NPs). The nanoparticles enzyme mimetic activity fits well the Michaelis–Menten equation, which make PB-Ft NPs a good reagent in glucose detection. The consequence of enzyme-linked immunosorbent assay (ELISA) reveals the specificity of ferritin was preserved in PB-Ft NPs and it makes PB-Ft NPs a useful mimic enzyme label in biomedical detection.

2. MATERIALS AND METHODS

2.1. Materials

All chemicals used in this experiment were of analytical reagent grade. Deionized water was used throughout the study. Horse spleen ferritin (HoSF), anti-horse spleen ferritin antibody (anti-HoSF), 3,3′,5,5′- tetramethylbenzidine (TMB) and 2,2′-Azinobis-(3-ethylbenzthiazoline-6-sulphonate) (ABTS) were bought from Sigma Aldrich Co. Ltd. (USA). Dimethyl sulfoxide (DMSO), glacial acetic acid, anhydrous sodium acetate, citric acid monohydrate, sodium sulfite, hydrochloric acid, hydroxylammonium chloride, 1,10-phenanthroline, dimethylbenzene, nutral balsam and ethyl alcohol were purchased from Sinopharm Chemical Reagent Co., Ltd. (China). Hydrogen peroxide (30%), glucose and glucose oxidase (GOx) were obtained from Aladdin Co., Ltd. (China). Sodium phosphate dibasic and potassium hexacyanoferrate were reagents from Shanghai Lingfeng Chemical Reagent Co., Ltd. (China). Sodium bicarbonate was purchased from Shanghai Hongguang Chemical Factory Co., Ltd. (China). Sodium hydroxide was obtained from Guangzhou Guanghua Chemical Factory Co., Ltd. (China). Bovine Serum Albumin (BSA) was obtained from Nanjing Bookman Biotechnology Ltd. (China).

2.2. Synthesis and Characterization of PB-Ft NPs

In our experiment, an optimal molar ratio of $K_4Fe(CN)_6$/HoSF = 0.75:1 was used to synthesize PB-Ft NPs. 20 μL of 47 mg/mL HoSF was mixed with 20 mL HCl solution (pH = 3.0), the concentration of iron (III) contained in the iron oxide cores is approximately 0.025 M in this mixture; 150 μL 0.025 M $K_4Fe(CN)_6$ was added to the former solution under stirring, then the solution was moved to 4 °C for 12 h. After that, PB-Ft NPs were obtained after dialysis and kept under 4 °C for later experiments. The synthesis procedure is as illustrated in Figure 1.

The morphology and particle size of PB-Ft NPs were characterized by transmission electron microscopy (TEM, JEOL JEM-2100) at 120 kV. Dynamic light scattering (DLS) together with a Particle Sizing Analyzer (Brookhaven, Zeta Plus) were used to determine hydrodynamic size distribution of the nanoparticles.

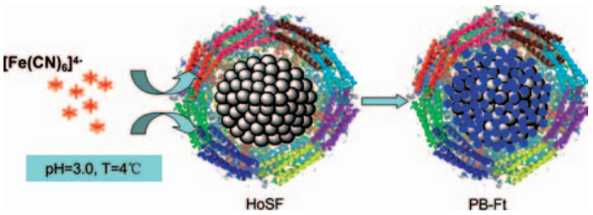

Fig. 1. Schematic illustration of the synthesis route of PB-Ft NPs. The reaction of $K_4Fe(CN)_6$ with iron (III) on the iron oxide core give rise to the formation of PBNPs within the ferritin cavity.

Shimadzu UV-3600 UV-VIS-NIR spectrophotometer was used to measure the Ultraviolet-visible (UV-vis) absorption spectra of the nanoparticles.

2.3. Peroxidase-Like Activity of PB-Ft NPs

2.3.1. Test of Peroxidase-Like Activity of PB-Ft NPs

The catalytic experiment of PB-Ft NPs was carried out at room temperature in a reaction system with 400 μL 0.05 mg/mL PB-Ft NPs in 4 mL NaAc-HAc buffer (pH = 3.6) in the presence of 320 μL 10 mg/mL TMB (or ABTS) and 640 μL 30% H_2O_2 as substrates. The absorbance values of the reaction systems catalyzed by PB-Ft NPs were recorded for 10 min with the microplate reader.

2.3.2. The Michaelis–Menten Kinetic Analysis

Steady-state kinetic assays were carried out at 25 °C with 10 μL 0.05 mg/mL (the ferritin concentration) PB-Ft NPs in 200 μL NaAc-HAc buffer (0.2 M, pH = 3.6) in the presence of H_2O_2 and TMB (or ABTS) in 96-well plates. The kinetic analysis of TMB (or ABTS) as the substrate was performed by adding 32 μL 30% H_2O_2 and different amounts (0, 0.5, 1, 2, 4, 6, 8, 10 μL) of TMB solution (10 mg/mL, dissolved in DMSO) or ABTS solution (10 mg/mL, dissolved in deionized water). The kinetic assay of H_2O_2 as the substrate was performed by adding 10 μL TMB and different amounts (2, 4, 8, 12, 16, 32, 64 μL) of 1% H_2O_2 solution, or 10 μL ABTS and different amounts (2, 4, 8, 12, 16, 32, 64 μL) of 0.05% H_2O_2 solution. All the reactions were detected at 650 nm for TMB or 415 nm for ABTS using the microplate reader. Catalytic parameters were determined by fitting the absorbance data to the Michaelis–Menten equation as Eq. (1), which describes the relationship between the rates of substrates conversion by PB-Ft NPs and the concentration of the substrates.

$$V = \frac{V_{\max}[S]}{K_m + [S]} \quad (1)$$

In this equation, V is the rate of conversion, $V_{\max}$ is the maximum rate of conversion, $[S]$ is the concentration of substrate and K_m is the Michaelis constant. The physical

RESEARCH ARTICLE

meaning of the Michaelis constant K_m is the substrate concentration at which the rate of conversion is half of V_{max}, enzymes with smaller K_m have higher affinity with the substrates.

2.3.3. PB-Ft NPs Concentration, pH and Temperature Dependence of Peroxidase-Like Activity

The catalytic reaction was carried under different pH, temperatures and PB-Ft NPs concentration. PB-Ft NPs concentration was from 1.012 μg/mL to 7.092 μg/ml, the pH changed from 2 to 11, the temperature increased gradually from 10 °C to 75 °C. According to the colorimetric reaction of TMB and ABTS oxidized by H_2O_2, these dependences were recorded by the absorbance value of the reaction systems using Shimadzu UV-3600 UV-VIS-NIR spectrophotometer.

2.4. Glucose Detection

Glucose detection was performed as follows: (a) 100 μL of glucose of different concentrations was incubated at 37 °C for 45 min with 100 μL 0.58 mg/mL GOx in 100 μL PBS (pH = 7.4); (b) 100 μL ABTS and 150 μL PB-Ft NPs in 450 μL Na_2HPO_4–$C_6H_8O_7$ buffer (pH = 3.0) were then added in, the solution was incubated at 40 °C for 45 min; (c) Finally, the absorbance at 415 nm of the mixed solution was measured by the UV-VIS-NIR spectrophotometer.

2.5. Enzyme-Linked Immunosorbent Assay (ELISA)

The specific targeting ability of PB-Ft NPs was verified by the ELISA. The experiment was carried out in 48-well plates, 100 μL of 10 μg/mL anti-HoSF in PBS buffer (pH = 7.4) was coated to the well surface at 37 °C for 1 h and then kept at 4 °C for 12 h, next, the wells were washed three times with PBS-T (pH = 7.4, Tween-20 0.05 volume %), each for 5 min. After that, the plate was blocked with 150 μL 1% BSA per well at 37 °C for 2 h to prevent the non-specific binding of immunoglobulins, the wells were then washed again with PBS-T as described before and added with 100 μL PB-Ft NPs. (The control-1 and the control-2 group were obtained by identical treatment with 100 μL PBS and HoSF, instead of PB-Ft NPs), after incubated at 37 °C for 2 h and washed by PBS-T for three times, the wells were filled with chromogenic substrate TMB and H_2O_2, and the absorbance at 650 nm was measured by a microplate reader (Elx 808, USA). In the study, concentration dependency of peroxidase-like activity was measured by diluting PB-Ft NPs in HCl (pH = 3.0) at doubling dilutions (1:2, 1:4, 1:8, 1:16, 1:32, 1:64), high and low anti-HoSF levels (1 μg/mL, 2.5 μg/mL, 5 μg/mL, 10 μg/mL) using to coat the well were also discussed in this study.

3. RESULTS AND DISCUSSION

3.1. Characterization of PB-Ft NPs

The obtained PB-Ft NPs display similar inner core morphology to the pure ferritin, as shown in TEM images (Figs. 2(a), (c)). From the TEM image negatively-stained with 2% phosphotungstic acid, it can be observed that the size and morphology of the ferritin shell remained the same with ferritins before reaction (Fig. 2(b), (d)), which indicated that the synthesis process of the PBNPs did not change the size and morphology of the hollow spherical shell of ferritin. From the high-resolution TEM (HRTEM) images (insets of Fig. 2(a), (b)) we found that the crystal structure of the iron oxide cores was disrupted to some extent after the reaction, however, the images show the regular lattice fringes remained 0.25 nm, which is relative to the (110) planes of ferrihydrite.[35] UV-vis absorption spectra of PB-Ft NPs in water (Fig. 3) presented PB's characteristic peak at approximately 700 nm[36] and the absorption of ferritin at 280 nm, resulting from the formation of PBNPs in the presence of ferritin. Note that, no individual Prussian blue particles were observed in the TEM sample, as shown typically in Figure 2(c). Therefore, it could be deduced that Prussian blue was deposited on the surface of the iron oxide cores rather than formed in reaction solution, but it was hardly distinguished from iron oxide due to low crystallinity and very small size. Dynamic light scattering analysis demonstrated that the HoSF dissolved in aqueous solution of pH = 3.0 have a mean size of 10.9 nm (Fig. 2(e)), which is close to the diameter of HoSF, indicating ferritin is monodispersed. After modification with PB, the sizes of the nanoparticles increased to 22.8 nm (Fig. 2(f)), attributed likely to the aggregation of the formed PB-Ft NPs induced by surface PB deposition and charge variation. Zeta potential of HoSF is +23.8 mV in pH 3.0, according with the fact that HoSF has an isoelectric point (IEP) at pH 5.8–6.[37] Whereas zeta potential of PB-Ft NPs is +13.7 mV, indicating that the negative charge of PB coated on the iron oxide cores reduced the positive charge of HoSF.

3.2. The Peroxidase-Like Activity of PB-Ft NPs

The peroxidase-like activity of PB-Ft NPs was evaluated through a colormetric reaction using TMB or ABTS as substrates in the presence of H_2O_2. As shown in Figure 4(A), the obvious color changes can be seen when PB-Ft NPs were used as catalyst. The absorbance change of oxidized products of substrates was also monitored with reaction time using HoSF and PB-Ft NPs as catalysts (Figs. 4(B), (C)). HoSF displays almost no peroxidase-like activity when the chromogenic substrate is TMB but weak activity when using ABTS as chromogenic substrate. The reason may be that ferritins are electropositive and ABTS is negatively charged while TMB is positively charged in NaAc-HAc buffer (pH = 3.6), resulting in the

RESEARCH ARTICLE

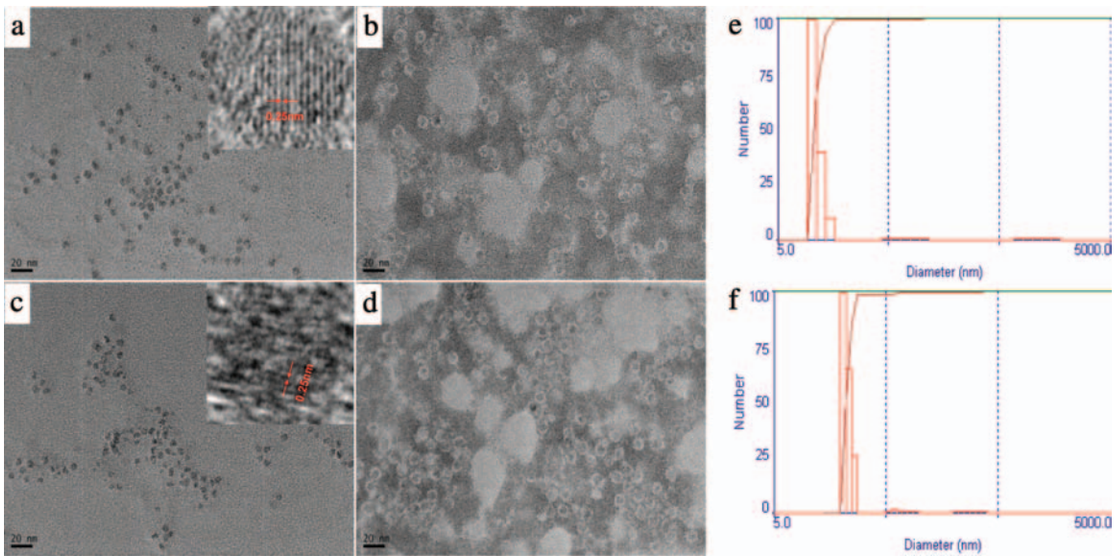

Fig. 2. Characterization of PB-Ft NPs and pure ferritin. (a) TEM photograph of unstained ferritin (inset: HRTEM image of ferritin). (b) Negatively-stained TEM photograph of ferritin. (c) TEM photograph of unstained PB-Ft NPs (inset: HRTEM image of PB-Ft NPs). (d) Negatively-stained TEM photograph of PB-Ft NPs. (e) Hydrodynamic size distribution of ferritin (average diameter is 10.9 nm). (f) Hydrodynamic size distribution of PB-Ft NPs (average diameter is 22.8 nm).

electrostatic adsorption between ferritin and ABTS and thus the enhanced catalytic oxidation of ABTS, where the iron oxide core of ferritin plays likely a weak catalytic role. For comparison, the intensive absorbance variation was observed when using PB-Ft NPs as catalyst, indicating the high peroxidase-like activity is contributed by the modification of PB.

The peroxidase-like activity of PB-Ft NPs was also investigated by determining the apparent steady-state kinetic parameters of the catalytic reaction. With a suitable range of H_2O_2 concentrations, typical Michaelis–Menten curves were observed for TMB (Fig. 5(a)) and ABTS (Fig. 5(b)). With a certain range of TMB and ABTS concentrations, the Michaelis–Menten curves were observed for H_2O_2 (Fig. 5(c), (d)). The data were fitted to the Michaelis–Menten model to obtain the parameters (Table I). The apparent K_m values of PB-Ft NPs with ABTS as substrate is much smaller than TMB, suggesting

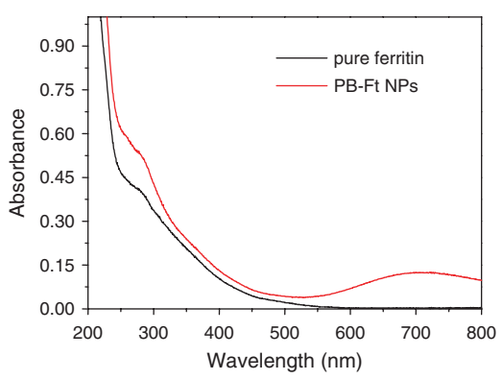

Fig. 3. UV-vis absorption spectra of ferritin and PB-Ft NPs.

that PB-Ft NPs have a higher affinity to the substrate ABTS than TMB due likely to the existence of a strong electrostatic interaction between ABTS and PB-Ft NPs, as indicated above. Table I gives the obtained apparent steady-state kinetic parameters. The previously reported PBMNPs (~10 nm) are also listed for comparison. The K_m value of PB-Ft NPs using TMB as substrate is higher than that for PBMNPs, suggesting that the PB-Ft NPs have lower affinity for TMB than PBMNPs; the K_m value of PB-Ft NPs with H_2O_2 as substrate is much lower than PBMNPs, indicating PB-Ft NPs are much more affinity to H_2O_2 than PBMNPs, which makes it a good reagent in H_2O_2 detection. The k_{cat} value of the PB-Ft NPs with TMB and H_2O_2 are both smaller than that for PBMNPs, originating from that ferritin shell leads to the lower exposure of PB active surface compared with PBMNPs. However, the k_{cat} value of PB-Ft NPs is two orders of magnitudes higher than Fe_3O_4 NPs (~10 nm) reported by Yang's group.[9, 38]

The peroxidase-like activity of PB-Ft NPs were also measured at different conditions using pH from 2 to 12, the temperature from 10 °C to 75 °C and the nanoparticle concentration from 1 μg/mL to 7 μg/mL. The results show the catalytic activity of PB-Ft NPs is dependent on pH, temperature and catalyst concentration (Fig. 6). The optimal pH was approximately 3.0 when the substrate is TMB, and the activity decreased with the increasing pH for ABTS (Figs. 6(a), (b)). The optimal temperature was 65 °C (Fig. 6(c)), implying a broader active temperature range than native enzyme. Figure 6(d) shows a linear absorbance increase with a correlation coefficient of 0.99 as a function of PB-Ft NPs concentration, indicating that PB-Ft NPs we prepared can be used as a peroxidase-like mimetics.

RESEARCH ARTICLE

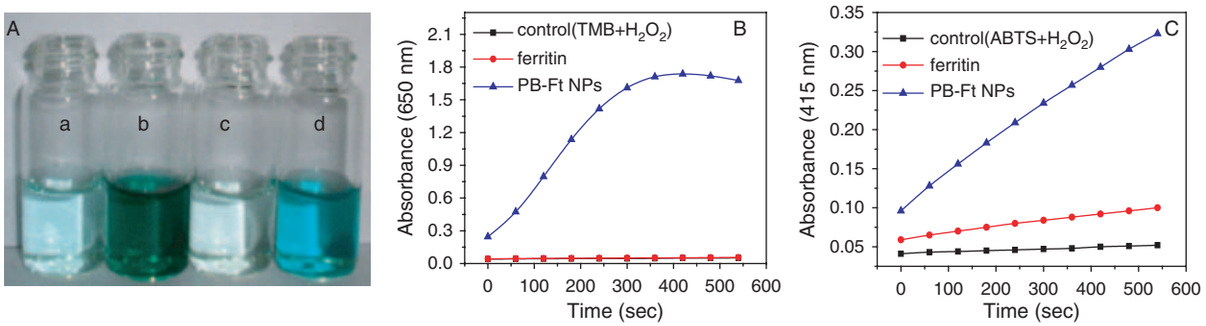

Fig. 4. PB-Ft NPs show peroxidase-like activity. A (a), (b), Reaction systems catalyzed without and with PB-Ft NPs using ABTS as chromogenic substrate. c, d Reaction systems catalyzed without and with PB-Ft NPs using TMB as chromogenic substrate. (B), (C), UV-vis absorbance-time curves of reaction systems catalyzed by PB-Ft NPs in the same buffer (HAc-NaAc solution, pH = 3.6) using TMB and ABTS as chromogenic substrates. The substrate oxidation reaction taking PBS (black lines) and HoSF (blue lines) instead of PB-Ft NPs was used as contrasts.

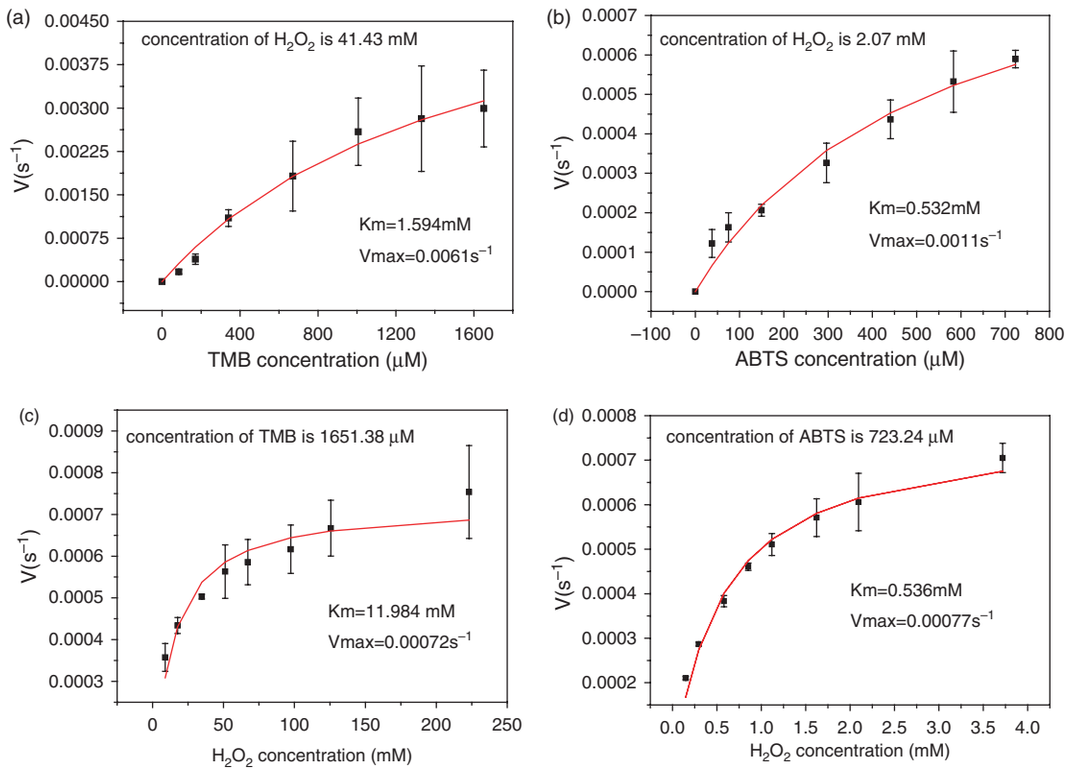

Fig. 5. Steady-state kinetic assay of PB-Ft NPs. The velocity (V) of the reaction was measured using 10 μL PB-Ft NPs in 200 μL HAc-NaAc buffer (pH = 3.6) at 25 °C. (a) The concentration of H_2O_2 was 41.43 mM and the TMB concentration was varied. (b) The concentration of H_2O_2 was 2.07 mM and the ABTS concentration was varied. (c) The concentration of TMB was 1651.38 μM and the H_2O_2 concentration was varied. (d) The concentration of ABTS was 723.24 μM and the H_2O_2 concentration was varied. The reaction velocity was calculated from the initial slopes of absorbance versus time curves.

3.3. Glucose Detection

Hydrogen peroxide is the main product in the glucose oxidase catalyzing reaction in the presence of glucose and oxygen.[39] On the basis of the peroxidase-like activity of PB-Ft NPs presented before, we designed a colorimetric glucose detection method by detecting the H_2O_2 generated in GOx catalyzed oxidation of glucose. As mentioned above, PB-Ft NPs displayed higher affinity to H_2O_2 when the chromogenic substrate was ABTS (Table I), so we measured the color change from ABTS to measure the concentration of glucose indirectly. Because GOx could be denatured in pH lower than 4.0, the detection was performed in two separate steps as described in experiment. As shown in Figure 7, the glucose can be detected as low as 0.39 μmol/L with the linear range of 0.39 μmol/L to 6.25 μmol/L. Because of high peroxidase-like activity and strong affinity to H_2O_2, the developed detection method

Table I. Kinetic parameters of PB-Ft NPs.

Catalyst	$[E]$/M	Substrate	K_m (mM)	V_{max} (Ms^{-1})	k_{cat}/s^{-1}	$(k_{cat}/K_m)/M^{-1}s^{-1}$
PB-Ft	7.22×10^{-10}	TMB	1.594	1.92×10^{-7}	2.66×10^{2}	1.7×10^{5}
	7.39×10^{-10}	H_2O_2 (TMB)	11.984	7.20×10^{-7}	3.13×10^{1}	2.6×10^{3}
	7.22×10^{-10}	ABTS	0.532	3.13×10^{-8}	4.32×10^{1}	8.6×10^{4}
	7.39×10^{-10}	H_2O_2 (ABTS)	0.537	6.14×10^{-9}	3.35×10^{1}	6.2×10^{4}
PBMNPs[9]	3.09×10^{-10}	TMB	0.307	1.06×10^{-6}	3.43×10^{3}	1.1×10^{6}
	3.09×10^{-10}	H_2O_2	323.6	1.17×10^{-6}	3.79×10^{3}	1.2×10^{4}

Notes: $[E]$ is the nanoparticle concentration, K_m is the Michaelis constant, V_{max} is the maximal reaction velocity and K_{cat} is the catalytic constant, where $k_{cat} = V_{max}/[E]$. Note that the k_{cat} value shows the catalytic efficiency per nanoparticle. PBMNPs represent PB coated Fe_2O_3 magnetic nanoparticles reported in our previous work.[9]

provides a lower detective concentration of glucose compared to carboxyl-modified graphene oxide (GO-COOH) (1 μmol/L)[39] and Fe_3O_4 nanoparticles (5 μmol/L).[40] And the slope of the fitted line can be regarded as the sensitivity to glucose, which is also much larger than the values in other literatures, indicating PB-Ft NPs are quite sensitive in glucose detection.

3.4. Enzyme-Linked Immunosorbent Assay (ELISA)

The principle of ELISA is the use of an enzyme to deliver a signal that a particular antigen-antibody reaction has occurred and to what extent. In our experiment, PB-Ft NPs were used as a probe with the simultaneous combination of the peroxidase-like activity of PB and the specificity of ferritin. Compared to the previously repored PBMNPs-SPA bioconjugates, PB-Ft NPs can effectively inhibit the non-specific adsorption owning to native ferritin shell. Figure 8(a) shows that the absorbance increases with nanoparticle concentration and reaches a pleatue when the concentration of PB-Ft NPs is approximately 4.0×10^{-11} mol/L, which was thus selected as a optimal probe concentration for anti-HoSF antibody detection. As shown in Figure 8(b), the HoSF group displays an absorbance slightly higher than the PBS group (control-1), the reason is that the iron oxide cores of ferritins presented weak catalytic activity, as indicated above. The competition group shows an absorbance higher than the HoSF group (control-2), a possible reason is the incubated PB-Ft NPs could not be totally washed off and gave rise to

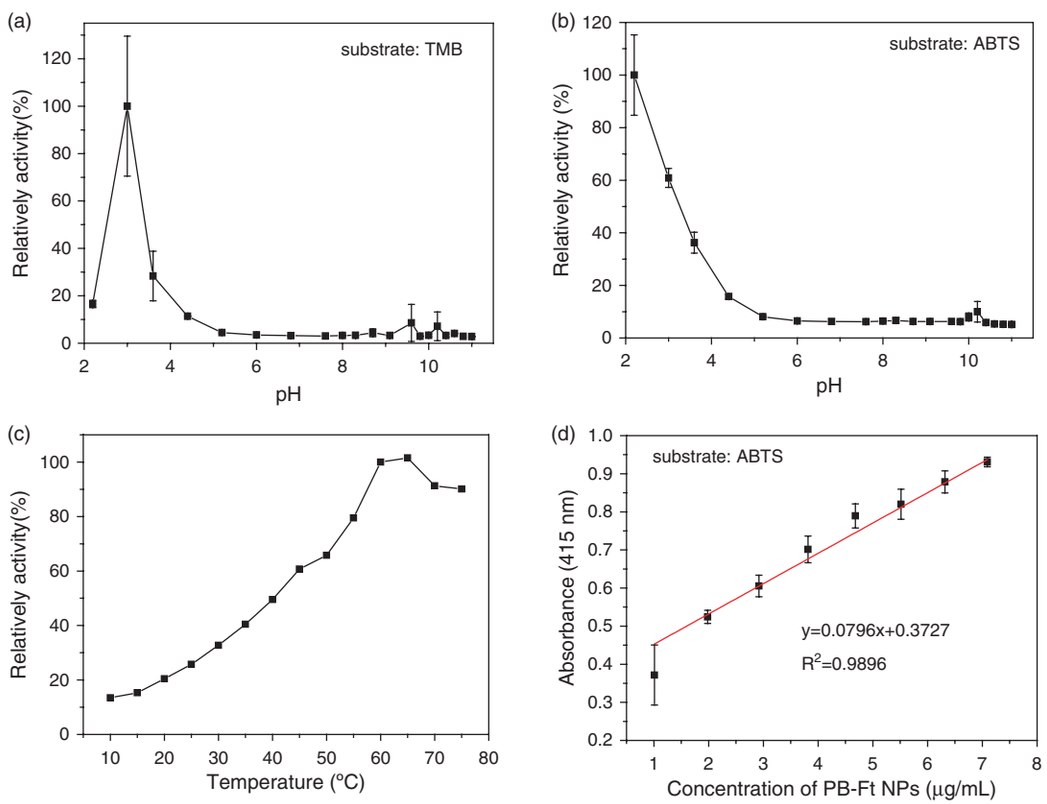

Fig. 6. The peroxidase-like activity of the PB-Ft NPs is pH (a, b), temperature (c), PB-Ft NPs concentration (d) dependent.

RESEARCH ARTICLE

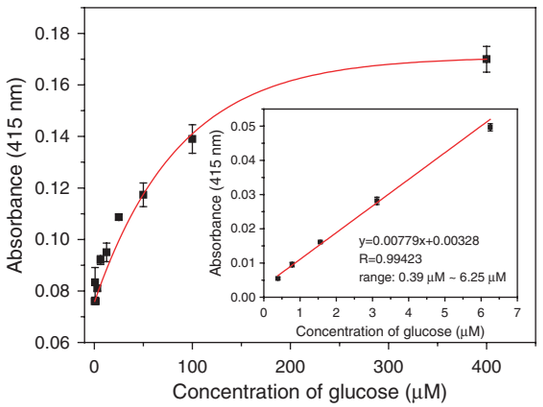

Fig. 7. A dose-response curve for glucose detection using GOx and PB-Ft NPs. Inset: linear calibration plot for glucose. The error bars represent the standard deviation of three measurements.

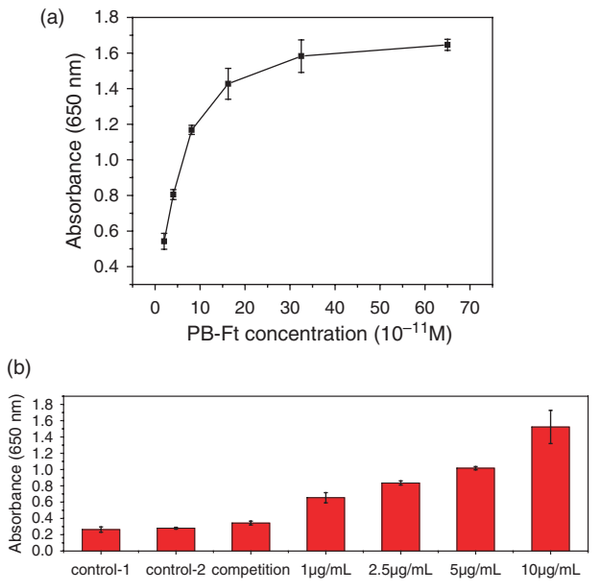

Fig. 8. Enzyme-linked immunosorbent assay based on both the peroxidase-like activity and the specificity of PB-Ft NPs. (a) Effect of PB-Ft NPs concentration on the detection of anti-HoSF (b) Immunoassays for the anti-HoSF antibody of different concentrations. The control groups using PBS (control-1) and HoSF (control-2) instead of PB-Ft NPs as well as the HoSF competition group were also carried out for comparison.

a inevitable catalytic reaction. PB-Ft NPs group shows a much higher absorbance which increases with the concentration of anti-HoSF antibody coated in the well, indicating PB-Ft NPs can specifically bind to the anti-HoSF antibody. Very currently, Yan's group[19] demonstrated that magneto-ferritin (M-HFn) nanoparticles synthesized by encapsulating iron oxide nanoparticles inside a HFn shell can target the overexpressed transferrin receptor 1 (TfR1) in tumour cells. It is expected that PB-Ft NPs, compared to Yan's work, may have higher efficiency due to the higher peroxidase-like activity of PBNPs than iron oxide nanoparticles.

4. CONCLUSIONS

In summary, a very simple and cheap template method to obtain PB-Ft NPs with very small size has been developed and the combining functions of the mimetic enzyme activity from PBNPs and the specificity of ferritin were realized. It has been demonstrated that the peroxidase-like activity of PB-Ft NPs is pH, temperature and PB-Ft NPs concentration dependent and fits well with typical Michaelis–Menten kinetics. PB-Ft NPs displayed quite high sensitivity and affinity to H_2O_2 with ABTS as choromogenic substrate, which makes PB-Ft NPs a good reagent in glucose detection. PB-Ft NPs were successfully used in the ELISA, indicating that in PB-Ft NPs the antibody binding functions of ferritin were preserved. These studies show this composite nanoparticle has potential application potential in bio-detection.

Acknowledgments: This research was supported by the National Important Science Research Program of China (Nos. 2011CB933503, 2013CB733800), National Natural Science Foundation of China (Nos. 31170959, 30970787), the Basic Research Program of Jiangsu Province (Natural Science Foundation, Nos. BK2011036, BK2009013), Research Fund for the Doctoral Program of Higher Education of China (20110092110029).

References and Notes

1. L. Z. Gao, J. Zhuang, L. Nie, J. B. Zhang, Y. Zhang, N. Gu, T. H. Wang, J. Feng, D. L. Yang, S. Perrett, and X. Y. Yan, *Nature Nanotech.* 2, 577 (**2007**).
2. H. D. Hill, R. A. Vega and C. A. Mirkin, *Anal. Chem.* 79, 9218 (**2007**).
3. S. Boland, F. Barriere, and D. Leech, *Langmuir* 24, 6351 (**2008**).
4. M. Nag, A. Patel, and N. M. Rao, *J. Biomed. Nanotechnol.* 7, 42 (**2011**).
5. M. M. Rahman, *J. Biomed. Nanotechnol.* 7, 351 (**2011**).
6. L. J. Xu, J. J. Du, Y. Deng, and N. Y. He, *J. Biomed. Nanotechnol.* 8, 1006 (**2012**).
7. F. Wang, C. Ma, X. Z., C. Y. Li, Y. Deng, and N. Y. He, J. *Biomed. Nanotechnol.* 8, 786 (**2012**).
8. J. Li, J. D. Qiu, J. J. Xu, H. Y. Chen, and X. H. Xia, *Adv. Funct. Mater.* 17, 1574 (**2007**).
9. X. Q. Zhang, S. W. Y. Gong, Y. Zhang, T. Yang, C. Y. Wang, and N. Gu, *J. Mater. Chem.* 20, 5110 (**2010**).
10. A. A. Karyakin, E. E. Karyakina, and L. Gorton, *Anal. Chem.* 72, 1720 (**2000**).
11. D. Ellis, M. Eckhoff, and V. D. Neff, *J. Phys. Chem.* 85, 1225 (**1981**).
12. G. C. Ford, P. M. Harrison, D. W. Rige, J. M. Smith, A. Treffry, J. L. White, and J. Yarriv, *Phil. Trans. R Soc. Lond.* 304, 551 (**1984**).
13. D. M. Lawson, P. J. Artymiuk, S. J. Yewdall, J. M. A. Smith, J. C. Livingstone, A. Treffry, A. Luzzzago, S. Levi, P. Arosio, G. Cesareni, C. D. Thomas, W. V. Shaw, and P. M. Harrison, *Nature* 349, 541 (**1991**).
14. M. V. Darl, P. M. Harrison, and W. Bottke, *Eur. J. Biochem.* 222, 367 (**1994**).
15. P. M. Harrison and P. Arosio, *Biochimica et Biophysica Acta* 1275, 161 (**1996**).
16. C. Q. Cao, L. X. Tian, Q. S. Liu, W. F. Liu, G. J. Chen, and Y. X. Pan, *J. Geophys. Res.* 115, B07103 (**2010**).

RESEARCH ARTICLE

17. C. J. Sun, H. Yang , Y. Yuan, X. Tian, L. M. Wang, Y. Guo, L. Xu, J. L. Lei, N. Gao, G. J. Anderson, X. J. Liang, C. Y. Chen, Y. L. Zhao, and G. J. Nie, *J. Am. Chem. Soc.* 133, 8617 **(2011)**.
18. M. Uchida1, M. Terashima, C. H. Cunningham, Y. Suzuki, D. A. Willits, A. F. Willis, P. C. Yang, P. S. Tsao, M. V. McConnell, M. J. Young, and T. Douglas, *Magn. Reson. Med.* 60, 1073 **(2008)**.
19. K. L. Fan, C. Q. Cao, Y. X. Pan, D. Lu, D. L. Yang, J. Feng, L. N. Song, M. M. Liang, and X. Y. Yan, *Nature Nanotech.* 7, 459 **(2012)**.
20. S. Aime, L. Frullano, and S. Geninatti, *Angewandte Chemie* 3, 1017 **(2012)**.
21. J. Fan, J. J. Yin, B. Ning, X. C. Wu, Y. Hu, M. Ferrari, G. J. Anderson, J. Y. Wei, Y. L. Zhao, and G. J. Nie, *Biomaterials* 32, 1611 **(2011)**.
22. J. M. D. Vera and E. Colacio, *Inorg. Chem.* 42, 6983 **(2003)**.
23. X. Lin, J. Xie, G. Niu, F. Zhang, H. K. Gao, M. Yang, Q. M. Quan, M. A. Aronova, G. F. Zhang, S. Lee, R. Leapman, and X. Y. Chen, *Nano Lett.* 11, 814 **(2011)**.
24. B. Hallgren and P. Sourander, *J. Neurochem.* 3, 41 **(1958)**.
25. K. D. Poss and S. Tonegawa, *Proc. Nat. Acad. Sci.* 94, 10919 **(1997)**.
26. K. D. Muirden and G. B. Senator, *Ann. Rheum. Dis.* 27, 38 **(1968)**.
27. M. C. Bessis and J. B. Gorius, *Blood* 19, 635 **(1962)**.
28. S. Levi, S. J. Yewdall, P. M. Harrison, P. Santambrogio, A. Cozzi, E. Rovida, A. Albertini, and P. Arosio, *Biochem. J.* 288, 591 **(1992)**.
29. J. W. M. Bulte, S. C. Zhang, P. V. Gelderen, V. Heryneki, E. K. Jordan, I. D. Duncan, and J. A. Frank, *Proc. Nat. Acad. Sci.* 96, 15256 **(1999)**.
30. D. L. Kraitchman, A. W. Heldman, E. Atalar, L. C. Amado, B. J. Martin, M. F. Pittenger, J. M. Hare, and J. W. M. Bulte, *Circulation* 107, 2290 **(2003)**.
31. A. S. Arbab, L. A. Bashaw, B. R. Miller, E. K. Jordan, B. K. Lewis, H. Kalish, and J. A. Frank, *Radiology* 229, 838 **(2003)**.
32. M. Schroeter, A. Saleh, D. Wiedermann, M. Hoehn, and S. Jander, *Magn. Reson. Med.* 52, 403 **(2004)**.
33. P. Jendelova, V. Herynek, L. Urdzikova, K. Glogarova, J Kroupova, B. Andersson, V. Bryja, M. Burian, M. Hajek, and E. Sykova, *J. Neurosci. Res.* 76, 232 **(2004)**.
34. U. I. Tromsdorf, O. T.Bruns, S. C. Salmen, U. Beisiegel, and H. Weller, *Nano Lett.* 9, 4434 **(2009)**.
35. N. D. Chasteen and P. M. Harrison, *J. Struct. Chem.* 126, 182 **(1999)**.
36. M. Pyrasch and B. Tieke, *Langmuir* 17, 7706 **(1999)**.
37. A. Passaniti and T. F. Roth, *Biochem. J.* 258, 413 **(1989)**.
38. F. Q. Yu, Y. Z. Huang, A. J. Cole, and V. C. Yang, *Biomaterials* 30, 4716 **(2009)**.
39. Y. J. Song, K. G. Qu, C. Zhao, J. S. Ren, and X. G. Qu, *Adv. Mater.* 22, 2206 **(2010)**.
40. H. Wei and E. K. Wang, *Anal. Chem.* 80, 2250 **(2008)**.

Received: 8 September 2012. Accepted: 4 October 2012.

RESEARCH ARTICLE